

SUPPLEMENTAL INFORMATIONS

Modeling Diastolic Dysfunction in Induced Pluripotent Stem Cell-Derived Cardiomyocytes from Hypertrophic Cardiomyopathy Patients

Haodi Wu^{1,2,3,*}, Huaxiao Yang^{1,2,3}, June-Wha Rhee^{1,2,3}, Joe Z. Zhang^{1,2,3}, Chi Keung Lam^{1,2,3},
Karim Sallam^{1,2,3}, Alex CY Chang^{1,4}, Ning Ma^{1,2,3}, Jaecheol Lee^{1,2,3}, Hao Zhang^{1,2,3},
Helen Blau^{1,4}, Donald M. Bers⁵, Joseph C. Wu^{1,2,3,*}

¹Stanford Cardiovascular Institute; ²Department of Medicine, Division of Cardiology; ³Institute for Stem Cell Biology and Regenerative Medicine; ⁴Baxter Laboratory for Stem Cell Biology, Department of Microbiology and Immunology, Stanford University School of Medicine, Stanford, CA 94305, USA; ⁵Department of Pharmacology, University of California, Davis, CA 95616, USA

***Corresponding authors:**

Joseph C. Wu, 265 Campus Drive, Room G1120, Stanford, CA 94305-5111. Tel: +01- 650-736-2246, E-mail: joewu@stanford.edu, or Haodi Wu, 265 Campus Drive, Room G1105, Stanford, CA 94305-5101. Tel: +01- 650-724-9240, E-mail: haodi@stanford.edu

SUPPLEMENTAL METHODS

Reprogramming of iPSCs. To generate patient-specific iPSC lines, peripheral blood mononuclear cells (PBMCs) were isolated from blood samples as described.¹ Briefly, the 4 Yamanaka factors were over-expressed in PBMCs using the Sendai virus vector.^{2,3} Single clones could be observed and selected after 1 week of transfection. Normally, 10 clones were selected for each patient cell lines, and kept in culture to passage 10 for karyotyping and pluripotency analysis. Qualified iPSC lines were banked in liquid nitrogen.

Differentiation of iPSC-CMs. All iPSC lines were kept in culture until passage 20 before differentiation. For passaging, iPSC culture was dissociated with Accutase (Innovative Cell Technologies) at 37°C for 5-10 min, and suspended iPSCs were reseeded on Matrigel-coated plates (BD Biosciences, San Jose, CA) at a density of 100-200K cells per well in 6-well plates. For differentiation, human iPSCs were kept in 6-well plates until they reach > 80% confluence.⁴ The medium was switched to RPMI 1640 with Insulin minus B27 supplement (Gibco®, Life Technology). The cells were treated with 6 μM CHIR99021 (Selleckchem.com) in RPMI + B27 (minus insulin) medium for 2 days, and then allowed to recover for 1 day with fresh RPMI + B27 (minus insulin) medium. After the medium change, cells were treated with 5 μM IWR-1 (Sigma) for 2 days, and placed in fresh RPMI + B27 (minus insulin) medium for another 2 days. Cells were then switched to RPMI + B27 (plus insulin) medium for 2 days. Beating iPSC-CMs were observed at 9-11 days after differentiation. To purify the iPSC-CMs, cardiomyocytes were stressed with glucose-free RPMI + B27 (plus insulin) medium for 2-3 rounds. Normally, the iPSC-CM culture achieved >90% TNNT2 positive cells by FACS assessment after purification steps. For all experiments, we used iPSC-CMs derived from 2 clones of each patient-specific iPSC line.

Differentiated iPSC-CMs were maintained in culture until day 30 before all expression and functional analyses. Data from 9 lines of iPSC-CMs were presented as the following groups: Ctrl (two healthy individuals), MYH7 (two patients with MYH7 R663H mutation), MYBPC3 (two patients with MYBPC3 V321M and MYBPC3 V219 mutations), TNNT2 (two patients with TNNT2 R92W mutation), and HCM with no DD (one patient with MYBPC3 c.2905+1G>A mutation). (**Table S1**)

Immunofluorescence staining. Culture cells were fixed with 4% paraformaldehyde (PFA)/PBS for 15 min, and then cells were permeabilized with 0.2% Triton X-100/PBS for 1 hour and blocked with 5% BSA in 0.2% Triton X-100/PBS for 2 hours. The primary antibodies used in these studies are cardiac troponin T (cTNNT2, Abcam), sarcomeric α -actinin (Sigma Aldrich), Nanog (Santa Cruz), OCT4 (Abcam), and DAPI (Molecular Probes).² Fluorescently labeled cells were examined and imaged with a confocal microscope (Carl Zeiss, LSM 510 Meta, Göttingen, Germany) at 20X to 63X objectives as appropriate.

Fura-2 ratiometric Ca²⁺ imaging in iPSC-CMs. Ctrl and HCM iPSC-CMs were dissociated with TrypLE™ Select Enzyme (10X) (Thermo Fisher) and re-seeded in Matrigel-precoated (BD Bioscience) 24×50 mm coverslips (Warner Instrument). After recovery for 2-3 days, cells were loaded with 5 μ M Fura-2 AM with 0.1% F-127 for 10 min at RT in Tyrode's solution (140 mM NaCl, 1 mM MgCl₂, 5.4 mM KCl, 1.8 mM CaCl₂, 10 mM glucose, and 10 mM HEPES, pH = 7.4 with NaOH at RT). Field stimulation at 0.5 Hz was used to pace the iPSC-CMs. Single cell Ca²⁺ handling was observed with a Nikon Eclipse Ti-E inverted microscope mounted with a 40× oil immersion objective (NA 0.95). Lambda DG-4 ultra-high-speed wavelength switching light source

(Sutter Instrument) was used to excite Fura-2 at 340 nm and 380 nm wavelength. Emission signals >510 nm wavelength were collected with iXon Ultra 897 EMCCD (Andor) as high-frame rate video (512×512, 50 fps). For SOCE recording, Ctrl and HCM iPSC-CMs were bathed in Ca²⁺-free buffer with 10 μM SERCA inhibitor CPA for 10 min and then were switched immediately to 1.8 mM Ca²⁺ buffer, and the intracellular Ca²⁺ influx was recorded with iXon Ultra 897 EMCCD (Andor) as a low-frame rate video (512×512, 0.5 fps) for 20 min. [Ca²⁺]_i signals were calculated as 340/380 ratio pairs. Raw imaging data were analyzed with customized MATLAB (MathWorks) scripts.

Sarcomere shortening measurement. The sarcomere structure of patterned iPSC-CMs (see below under traction force microscopy for details regarding cardiomyocyte patterning) was labeled with GFP-conjugated actin using the Baculovirus vector (BacMam 2.0, CellLight® Actin-GFP, ThermoFisher Scientific, C10582). After 2-3 days following transfection, beating iPSC-CMs were examined using a confocal microscope (Carl Zeiss, LSM 710, Göttingen, Germany) with a 63X oil immersed objective (Plan-Apochromat 63x/1.40 Oil DIC M27). Sarcomere shortening was recorded as time-lapse line scanning (10 ms per line, 512 pixels*1920 lines) along the longitudinal axis of patterned iPSC-CMs within the labeled sarcomere structure. Sarcomere shortening data were processed with fast Fourier transformation (FFT) function using a customized MATLAB (MathWorks) script.

RNA extraction and quantitative real-time PCR (qPCR). Total RNA of cultured iPSC-CMs was isolated using Qiagen miRNeasy Mini Kit (Qiagen Sciences, Inc, Germantown, MD). High Capacity RNA-to-cDNA kit (Life Technology) was used for the reverse transcription of 1 μg RNA

of each total RNA sample. 0.2 μ L of cDNA template, 1 μ L TaqMan[®] primer sets (Life Technology), 10 μ L of TaqMan[®] Master Mix (Life Technology), and 8.8 μ L ddH₂O were mixed as the reaction system, and real-time quantitative PCR reaction was monitored with CFX Real-Time PCR System (Bio-Rad). To minimize the variation, each sample was run in triplicate and was normalized to 18S rRNA level. All TaqMan primer sets used in the current study are summarized. (**Table S2**)

Fluorescence activated cell sorting (FACS) analysis of iPSC-CMs. Differentiated and purified iPSC-CMs were dissociated into single cells by TrypLE[™] (GIBCO 12605) for 10 min at 37°C. The cell pellet was collected by centrifugation, and then re-suspended with PBS. The cell suspension was fixed and permeabilized using BD Cytotfix/Cytoperm[™] Fixation/Permeabilization Solution Kit (BD 554714). For cell labeling, iPSC-CMs were incubated with mouse anti-human TNNT2 antibody (Thermo MS-295-P1, 1:200) overnight at 4°C, followed by Alexa Fluor[®] 488 conjugate goat anti-mouse IgG (H+L) secondary antibody (Life technologies A11029, 1:250) for 30 min on ice. Before sorting, the cell suspension was filtered through a cell strainer cap of FACS tube (Fisher Scientific 08-771-23) to remove cell clumps. After staining, cells were re-suspended in 500 μ L FACS buffer and loaded on a BD Biosciences FACS Aria II instrument fitted with a 100 μ m nozzle using FACSDiva software. The percentage of iPSC-CMs was calculated as the ratio of TNNT2⁺ cells in the whole population.

Traction force microscopy. Hydrogel-covered imaging chambers for traction force microscopy were prepared as described.⁵ Briefly, polymer solution (10% acrylamide, 0.1% N,N methylene-bis-acrylamide, 0.1% ammonium persulfate, and 0.1% of N,N,N',N'-Tetramethylethylenediamine) was allowed to polymerize between 35 mm glass bottom dishes (MatTek) and cover glasses to

form an even layer of hydrogel in imaging dish. The substrate was activated by incubating it in 0.2 mg/ml sulfo-SANPAH (Pierce) in 50 mM HEPES pH 8.5, followed by UV light exposure for 10 min. 0.1% (v/v) fluorescent microspheres (Life Technology, 0.2 μ m 580/605) in PBS were added to the dishes, which were embedded into the surface of the hydrogel. Then, the dishes were coated with Matrigel overnight. Ctrl and HCM iPSC-CMs were seeded on the microsphere-embedded hydrogel dishes. Simultaneous recording of traction force microscopy and Ca^{2+} imaging was performed with a Nikon Spinning Disk confocal system (Nikon TiE inverted microscope, PLAN APO, 60x, N/A 1.40, oil immersion objective). For Ca^{2+} indication, cells were loaded with 5 μ M Fluo-4 AM in Tyrode's solution for 5-10 min at 37°C. Ca^{2+} handling (Em 505 nm) and fluorescent microsphere displacement signals (Em 605 nm) were separated by a GFP/mCherry filter in the Tu-Cam light splitter system (Andor) to be captured by two iXon Ultra 897 EMCCDs (Andor) as high-frame rate videos (512*512, 30 fps). For analysis of the Ca^{2+} data, a custom-made script based on IDL (Interactive Digital Language) was used. Ca^{2+} signal intensity was normalized to the intracellular basal level (F_0), and its transient amplitude was expressed as $\Delta F/F_0$. Traction force microscopy was performed using a particle image velocimetry script in MATLAB (MathWorks) as previously described.⁶ All reported forces generated during cell contraction are relative to the resting state of the cell between contractions.

Protein extraction and western blot. For protein extraction, iPSC-CMs were homogenized in a RIPA buffer with cOmplete™ Protease Inhibitor Cocktail (Roche) and centrifuged at 12,000 rpm, 4°C for 10 min to remove cell debris. Protein concentration in the supernatant was quantified with Pierce™ BCA Protein Assay Kit (Pierce Biotechnology Inc.). For western blotting, 50 μ g of protein was separated by NuPAGE® Novex® 4-12% Bis-Tris Protein Gel (Invitrogen, Carlsbad, CA) at

120V for 30 min. After transfer to Invitrolon™ PVDF Blotting Membranes (ThermoFisher Scientific), the protein lanes were analyzed by western blot using specific antibodies against CaMKII (pThr286 or 287), CaMKII δ (Badrilla). GAPDH was used as loading control. The signal intensity of the bands was analyzed and quantified with ImageJ Fuji program.

Cell apoptosis assay. For apoptosis assay, iPSC-CMs from both Ctrl and HCM groups were plated in 96-well plates at a density of 100-200 K cells per well. Cells in baseline groups were replaced with fresh RPMI + B27 medium every day, while ISO treatment groups were treated with 100 nM of ISO daily for 7 days. The working concentrations of other drugs in the study were: 10 nM verapamil, 10 nM diltiazem, 10 μ M ranolazine, 1 μ M metoprolol, 1 μ M carvedilol, and 300 nM doxorubicin. Each treatment group was run in triplicates to eliminate variance. Caspase activity were measured at the end of 7 days of continuous treatment with Caspase-Glo® 3/7 Assay Systems (Promega) following the manufacturer's instructions. Briefly, equal volumes of Caspase-Glo mixture reagent were added to each well of cells, and then incubated for 1 hr before bioluminescence measurement.

Gain and loss-of-function study of CaMKII δ in iPSC-CMs. For overexpression of CaMKII δ T287D in Ctrl iPSC-CMs, the plasmid sets encoding both constitutively activated and wild-type human CAMK2D were generously provided by Dr. Mark Anderson (Johns Hopkins University) as gifts. Highly concentrated and pure plasmids (~1 μ g/ μ l) were extracted with endotoxin-free Maxi plasmid prep kit (Qiagen). For siRNA-mediated knockdown of CaMKII δ in HCM iPSC-CMs, the siRNA sets for CaMKII δ (Assay ID: s2366) and scrambled siRNA (AM4611) controls were obtained from Thermo Fisher. Ctrl and HCM iPSC-CMs were seeded in 12-well plates and

8-well chambered coverslips (LabTek 155409). After recovery for 3~4 days, the Ctrl iPSC-CMs were transfected with target plasmid using GeneJammer reagent according to the manufacturer's protocol (Agilent Technologies 204132), and HCM iPSC-CMs were transfected with either scrambled or CaMKII α -targeting siRNA using Lipofectamine RNAiMAX according to the manufacturer's protocol (Thermo Fisher 13778075, Assay ID: s2366). The transfected cells were subjected to subsequent mRNA/protein expression profiling and functional analyses after 48 hr incubation in normal CM culture medium (RPMI+B27).

Generation of isogenic iPSC lines for TNNT2 R92W HCM mutation using CRISPR/Cas9.

To generate the isogenic iPSC lines by introducing the TNNT2 R92W mutation into Ctrl lines and correcting the mutation in HCM lines, we used pSpCas9(BB)-2A-GFP (PX458), a gift from Feng Zhang laboratory (Addgene plasmid # 48138), as the vector for genome editing. For the site-specific CRISPR/Cas9 and guide RNA sequence construction, two reverse complementary guide oligos were annealed first and then ligated to the linearized PX458 vector (**Supplemental Table 3**). The single-stranded oligodeoxynucleotides (ssODNs) template with designed mutation/correction sites were designed as previously described. Control and HCM iPSCs were dispersed the day before transfection at ~40-50% confluency as single cells. The next day, CRISPR/Cas9 and ssODN templates were transfected to the iPSCs using GeneJammer reagent according to the manufacturer's protocol (Agilent Technologies 204132). After 36 hours following transfection, GFP positive cells were sorted out using FACS and were seeded at a density of 2,000 cells/well in a 6-well plate. After expansion for about one week, single cell-derived colonies were observed and picked for genotype characterization and subsequent expansion. DNA was extracted from collected cells using QuickExtract solution (Epicenter). PrimeSTAR® GXL DNA

Polymerase (Clontech) was used for PCR amplification. The sequence of primers used for identifying the targeted sequences in TNNT2 are specified. (**Table S3**).

Statistical analysis. For statistical analysis, the Student's t-test was used to compare the difference between two data sets for normally distributed data; otherwise, the Mann–Whitney U test was used. For comparisons among multiple groups, one-way or two-way ANOVA was used where appropriate, and Holm-Sidak or Tukey after-tests was used for all pairwise comparisons, depending on the properties of the data sets. The sample size in each groups was determined by SigmaPlot estimations using margin of error (MOE) and SD, at a high power level (0.9). Detailed information of sample size and statistical analysis in each figures is summarized. (**Table S4**)

SUPPLEMENTAL FIGURE LEGENDS

Supplemental Figure 1. Differentiation of patient specific HCM iPSC-CMs. (A) Family pedigree trees of the HCM patients involved in the current study. Mutations are MYH7 R663H, MYBPC3 V321M, MYBPC3 V219L, TNNT2 R92W, and MYBPC3 c.2905+1 G>A. Recruited patients are boxed in red. (B) Representative immunostaining of the pluripotency markers of iPSC clones used in the study, including SOX2 (in green), OCT4 (in red), NANOG (in green), and SSEA-4 (in red). (C) Representative immunostaining of the sarcomere structures (TNNT2 in red and α -actinin in green) of differentiated Ctrl (left) and HCM (right) iPSC-CMs showing detailed sarcomere structures. (D) FACS analysis showing high purity of differentiated iPSC-CMs in Ctrl, HCM, and genome-edited groups, as indicated by the percentage of TNNT2⁺ cells, the first panel showed no TNNT⁺ cells in the iPSC control group.

Supplemental Figure 2. Recapitulation of diastolic dysfunction in patient specific HCM iPSC-CMs. Sarcomere shortening assays showed a trend toward prolonged contraction duration 90 (A), unchanged contractile velocity (B), beating rate (C), and significantly decreased fractional shortening (D) in all 3 groups of HCM iPSC-CMs compared to Ctrl iPSC-CMs. All groups were compared to Ctrl by one-way ANOVA (Tukey method). N = 42, 36, 40, and 44 cells in Ctrl, MYH7, MYBPC3, and TNNT2 groups, respectively. For each group, iPSC-CM data were generated from 2 different iPSC lines and 3 batches of differentiation.

Supplemental Figure 3. Optimization of Fura-2 AM ratiometric Ca²⁺ imaging. (A) Representative traces of Fura-2 AM based Ca²⁺ imaging in iPSC-CMs, paced from 0.5 HZ to 1.2 HZ. Red arrows indicate abnormal Ca²⁺ handling in the recordings. Statistical analysis showed

elevated diastolic Ca^{2+} concentration (**B**), unchanged peak Ca^{2+} concentration (**C**), and bigger variations in the beating regularity (**D**) in iPSC-CMs paced with higher frequency. All groups compared to 0.5 HZ by one-way ANOVA (Tukey method). N = 12, 16, 18, 10, and 11 cells in 0.5 HZ, 0.75 HZ, 0.8 HZ, 1 HZ, and 1.25 HZ groups, respectively. For each group, iPSC-CMs were from 1 Ctrl iPSC line and 2 batches of differentiation.

Supplemental Figure 4. iPSC-CMs from HCM patient without DD showed normal diastolic function. (**A**) Representative traces of Fura-2 AM based Ca^{2+} imaging in Ctrl iPSC-CMs and iPSC-CMs from an HCM patient with no clinical DD phenotype. (**B-E**) Statistical analysis of Ca^{2+} handling data showed minor decreases in diastolic Ca^{2+} concentration in HCM iPSC-CMs (**B**), while there were no significant changes in the transient rise time (**C**), transient rise rate (**D**), and normalized transient decay time (**E**) in iPSC-CMs from HCM patient with no DD compared to Ctrl group. All groups compared to Ctrl by Student's t-test. N = 163 and 152 cells in Ctrl and HCM groups. Data from 2 different Ctrl lines and 1 HCM line from 3 batches of differentiations. (**F-I**) Statistical analysis of sarcomere shortening data showed that there was no change of diastolic sarcomere length (**F**), beating rate (**G**), relaxation velocity (**H**), and relaxation duration (**I**) in HCM compared to Ctrl iPSC-CMs. All groups compared to Ctrl groups using Student' t-test. Data from >100 cells of 2 different Ctrl lines and 1 HCM line from 3 rounds of differentiations. All groups compared to Ctrl by Student's t-test. N = 46 and 51 cells in Ctrl and HCM groups. Data from 2 different Ctrl and 1 HCM lines and 2 batches of differentiations.

Supplemental Figure 5. Confirm the pathogenicity of HCM mutation using CRISPR/Cas9-edited isogenic Ctrl and HCM iPSC line. (**A**) Schematic diagram of genome editing strategy to

introduce TNNT2 R92W mutation into the Ctrl iPSC line. **(B-C)** gRNA and ssODN design for introduction and correction of TNNT2 R92W mutation in Ctrl and HCM iPSCs. Red boxes indicate the codon to be edited, red characters highlight the base to be replaced, blue boxes indicate the same-sense mutation in ssODNs design, and blue characters highlight mutated nucleotides. **(D-E)** Sequencing results showed successful heterozygous (C/T) and homozygous (T/T) introduction of the TNNT2 R92W mutation into Ctrl iPSC line (D), and successful correction of the mutation to wild type TNNT2 (C/C) in HCM iPSC line (E). **(F)** Representative traces of Ctrl, HCM, and genome-edited iPSC-CMs. **(G-I)** Calcium imaging showed that both C/T and T/T introduction of TNNT2 R92W in Ctrl iPSC-CMs greatly increased diastolic calcium ratio (G), decreased maximum transient rise rate (H), and prolonged the calcium decay time (I), while the mutation correction (C/C) showed opposite trends compared to HCM iPSC-CMs. Heterozygous (C/T) and homozygous (T/T) introduction groups compared to Ctrl by one-way ANOVA (Tukey method) and correction (C/C) group compared to HCM group by Student's t-test. N = 163, 127, 139, 129, and 123 cells in Ctrl, (C/T), (T/T), HCM, and (C/C) groups, respectively. Data were generated from 1 Ctrl, HCM or genome-edited line from 3 batches of differentiations. **(J-L)** Contractile function measurement suggested that both C/T and T/T introduction of TNNT2 R92W down-regulated the diastolic sarcomere length (J) and relaxation velocity (K), and decayed relaxation duration (L) in Ctrl iPSC-CMs, while the mutation correction has improved all these parameters in HCM iPSC-CMs. Heterozygous (C/T) and homozygous (T/T) introduction groups were compared to Ctrl by one-way ANOVA (Tukey method), correction (C/C) group were compared to HCM group by Student's t-test. N = 42, 62, 68, 44, and 78 cells in Ctrl, heterozygous (C/T), homozygous (T/T), HCM, and correction (C/C) groups, respectively. Data from 1 Ctrl, HCM or genome-edited line and 3 batches of differentiations.

Supplemental Figure 6. DCM and HCM iPSC-CMs showed opposite changes in Ca²⁺ sensitivity. (A) Representative traces of Fura-2 AM Ca²⁺ imaging in Ctrl, DCM, and HCM iPSC-CMs. (B) Diastolic Ca²⁺ was increased in HCM iPSC-CMs, but was unchanged in DCM iPSC-CMs compared to Ctrl group. (C-F) Simultaneous Ca²⁺ and traction force microscopy recording showed slightly increased contractile rates and significantly higher T-C gains in HCM iPSC-CMs. The Ca²⁺ transient and contractile stress amplitude were significantly decreased in DCM iPSC-CMs, resulting in slower contractile rate and reduced T-C gain, compared to Ctrl cells. All groups compared to Ctrl by one-way ANOVA (Tukey method). N = 74, 72, and 59 cells in Ctrl, HCM, and DCM groups, respectively. Data were generated from 2 different Ctrl, 2 HCM, and 1 DCM iPSC lines and 2 batches of differentiation.

Supplemental Figure 7. Short-term β -adrenergic stimulation exaggerated Ca²⁺ overload and slowed relaxation in HCM iPSC-CMs. (A) The effect of short-term isoproterenol (ISO) treatment on peak Ca²⁺ concentrations in Ctrl iPSC-CMs and HCM iPSC-CMs. (B) SR load measurement by caffeine-induced transient amplitude showed that short-term ISO treatment enhanced SR load in Ctrl but not HCM iPSC-CMs. All groups compared to baseline (without ISO treatment) groups by two-way ANOVA (Holm-Sidak method). N = 51, 47, 42, 41, 43, 33, 72, and 41 cells in Ctrl Base, Ctrl ISO, MYH7 Base, MYH7 ISO, MYBPC3 Base, MYBPC3 ISO, TNNT2 Base, and TNNT2 ISO groups, respectively. For all groups, data were generated from 2 different iPSC lines and 3 batches of differentiation. (C-D) Sarcomere shortening assay showed that short-term ISO treatment had no effect on the peak sarcomere length but prolonged the relative contraction duration (contraction duration 90 normalized to beating intervals) in HCM iPSC-CMs compared to Ctrl iPSC-CMs. All groups were compared to the baseline groups by two-way

ANOVA (Holm-Sidak method). N = 42, 33, 36, 30, 40, 28, 44, and 29 cells in Ctrl Base, Ctrl ISO, MYH7 Base, MYH7 ISO, MYBPC3 Base, MYBPC3 ISO, TNNT2 Base, and TNNT2 ISO groups, respectively. For all groups, data were from 2 different iPSC lines and 3 batches of differentiation.

Supplemental Figure 8. Treatment of HCM iPSC-CMs with Ca²⁺ and late Na⁺ channel blockers. (A) Representative traces of treatments with different doses of Ca²⁺ and late Na⁺ blockers (Verapamil, Diltiazem, Ranolazine, and Eleclazine), entresto, and Pyr3 on HCM iPSC-CMs. Note that a high dose of Ca²⁺ blockers will totally attenuate normal beating of iPSC-CMs. (B-D) Fura-2 Ca²⁺ imaging showed that treatment of HCM iPSC-CMs with both eleclazine and Pyr3 restored Ca²⁺ homeostasis in terms of reduced diastolic calcium ratio (B), slightly increased Ca²⁺ amplitude (C), and significantly shortened the calcium decay time (D). All groups were compared to HCM untreated groups by one-way ANOVA (Tukey method). N = 51, 72, 114, 94, and 100 cells in Ctrl Base, HCM Base, HCM Eleclazine, HCM Entresto, and HCM PYR3 groups, respectively. For all groups, data were from 2 different iPSC lines and 2 batches of differentiation. (E-G) Sarcomere shortening measurement showed that the eleclazine (elec) and Pyr3 treatments significantly retained the diastolic sarcomere length (E), relaxation velocity (F), and the relative relaxation durations (G) in HCM iPSC-CMs. Yet, no beneficial effect was observed with entresto (entre) treatment. All groups were compared to HCM untreated groups by one-way ANOVA (Tukey method). N = 42, 44, 36, 28, and 32 cells in Ctrl Base, HCM Base, HCM Eleclazine, HCM Entresto, and HCM PYR3 groups, respectively. For all groups, data were from 2 different iPSC lines and 2 batches of differentiation.

Supplemental Figure 9. Up-regulation of TRPCs contribute to the increase of SOCE in HCM iPSC-CMs. (A) Real-time PCR profiling of the mRNA expression level of key Ca^{2+} homeostasis-related proteins. All groups were compared to Ctrl by one-way ANOVA (Tukey method); data from 2 lines of Ctrl iPSC-CMs and 2 lines of HCM iPSC-CMs with each mutation of 2 batches of differentiations. (B) Comparison of the expression abundance of different cardiac hypertrophy-related TRPs. Data from 2 lines of Ctrl iPSC-CMs of 2 batches of differentiations. (C-E) Representative tracings of SOCE experiments in both Ctrl and HCM group at baseline (C), with Ca^{2+} channel and NCX blockers (verapamil and KB-R7943, to isolate TRPC dependent SOCE component) (D), and with Ca^{2+} channels, NCX and TRPC blockers (SKF-96265) (E). (F-H) HCM iPSC-CMs showed no changes in basal Ca^{2+} level in Ca^{2+} -free buffer (F), but showed significantly greater SOCE amplitude with and without Ca^{2+} and NCX blocker compared to Ctrl iPSC-CMs. All groups were compared to Ctrl treated with verapamil and KB-R7943 by two-way ANOVA (Tukey method). N = 50, 52, 52, 31, 54, 41, 106, and 34 cells in Ctrl Base, Ctrl treated, MYH7 Base, MYH7 treated, MYBPC3 Base, MYBPC3 treated, TNNT2 Base, and TNNT2 treated groups, respectively. For all groups, data were from 2 different iPSC lines and 2 batches of differentiation.

Supplemental Figure 10. Gain and loss-of-function study confirmed the key role of CaMKIId activation in calcium overload and DD development in HCM iPSC-CMs. (A-C) Expression profile showed significant up-regulation of CaMKIId mRNA and protein with both pCMV myc-CaMKIId wt (OE-WT) and pCMV myc-CaMKIId T287D (OE-CA) over-expression, while specific siRNA treatment (SI-CA) has markedly reduced the mRNA and protein expression of CaMKIId compared to scrambled siRNA (SI-NC). All OE groups were compared to Ctrl NC, and all SI groups were compared to HCM NC group in (C) by one-way ANOVA (Tukey method).

Data were generated from 2 different iPSC lines and 2 batches of differentiations for each group. **(D)** Representative Fura-2 AM Ca^{2+} imaging traces in Ctrl CaMKIId wt OE, Ctrl CaMKIId T287D OE, HCM scrambled siRNA, and HCM CaMKIId siRNA groups. **(E-G)** Calcium imaging data showed CaMKIId T287D OE increased diastolic calcium ratio (E), reduced transient rising rate (F), and prolonged transient decay time (G) in Ctrl iPSC-CMs, while CaMKIId KD rebalanced diastolic calcium (E) and restored calcium recycling in HCM iPSC-CMs. OE-CA compared to OE-WT group, and SI-CA compared to SI-NC group using Student's t-test. N = 52, 89, 73, and 64 cells in OE-WT, OE-CA, SI-NC, and SI-CA groups, respectively. For each group, data were generated from 2 different iPSC lines and 2 batches of differentiations. **(H-J)** Contractile function assay confirmed CaMKIId T287D OE impaired relaxation function in Ctrl iPSC-CMs, in terms of reduced diastolic sarcomere length (H), reduced relaxation velocity (I), and prolonged relaxation duration (J). CaMKIId KD restored the diastolic sarcomere length (H) and relaxation duration (J), thus has partially recovered the relaxation function in HCM iPSC-CMs. OE-CA were compared to OE-WT group, and SI-CA compared to SI-NC group using Student's t-test. N = 46, 45, 48, and 52 cells in OE-WT, OE-CA, SI-NC, and SI-CA groups, respectively. Data from 2 different iPSC lines and 2 batches of differentiations. **(K)** Luciferase based apoptosis assays indicated that CaMKIId T287D OE increased the cell death in Ctrl iPSC-CMs, both with and without long-term β -adrenergic challenge; while HCM iPSC-CMs were protected from cell death with CaMKIId KD in both conditions. All groups compared to Base groups by two-way ANOVA (Tukey method). For all groups, data were from 2 different iPSC lines and 2 batches of differentiation.

Supplemental Figure 11. Schematic diagram of the cellular mechanisms of diastolic dysfunction in HCM iPSC-CMs. In normal cardiomyocytes, Ca^{2+} influx through Ca^{2+} channels

activate Ryanodine receptors on sarcoplasmic reticulum (SR) via Ca^{2+} induced Ca^{2+} release mechanism (CICR), giving rise to the global Ca^{2+} increase as Ca^{2+} transient, and enabling the force generation in myofilament. In the diastole phase, Serca2a and NCX remove the free Ca^{2+} in the cytosol and facilitate the relaxation of sarcomeres. In HCM iPSC-CMs, enhanced Ca^{2+} sensitivity of myofilaments results in enhanced basal tension of cardiomyocytes, contributing to the overexpression and increased activity of TRPC channels on the cell membrane. More Ca^{2+} influx through TRPC channels in HCM iPSC-CMs results in elevated diastolic Ca^{2+} in the cytosol, increasing SR Ca^{2+} load and leak, and the activation of calmodulin and CaMKII signaling. CaMKII can further phosphorylate key proteins in Ca^{2+} handling, such as $\text{Ca}^{2+}/\text{Na}^+$ channels and phospholamban (PLN), resulting in the up-regulation of the Na^+ and Ca^{2+} influx during each beating cycle and further increasing the diastolic cytosol Ca^{2+} concentration and SR Ca^{2+} load. Together, increased diastolic Ca^{2+} and enhanced myofilament Ca^{2+} sensitivity contribute to the impaired relaxation of myofilaments. Moreover, prolonged Ca^{2+} overload in cytosol and increased CaMKII activity can lead to pro-apoptotic effect in HCM iPSC-CMs.

SUPPLEMENTAL REFERENCES

1. Fusaki N, Ban H, Nishiyama A, Saeki K, Hasegawa M. Efficient induction of transgene-free human pluripotent stem cells using a vector based on Sendai virus, an RNA virus that does not integrate into the host genome. *Proceedings of the Japan Academy Series B, Physical and biological sciences* 2009;**85**(8):348-62.
2. Sun N, Yazawa M, Liu J, Han L, Sanchez-Freire V, Abilez OJ, Navarrete EG, Hu S, Wang L, Lee A, Pavlovic A, Lin S, Chen R, Hajjar RJ, Snyder MP, Dolmetsch RE, Butte MJ, Ashley EA, Longaker MT, Robbins RC, Wu JC. Patient-specific induced pluripotent stem cells as a model for familial dilated cardiomyopathy. *Sci Transl Med* 2012;**4**(130):130ra47.
3. Lan F, Lee AS, Liang P, Sanchez-Freire V, Nguyen PK, Wang L, Han L, Yen M, Wang Y, Sun N, Abilez OJ, Hu S, Ebert AD, Navarrete EG, Simmons CS, Wheeler M, Pruitt B, Lewis R, Yamaguchi Y, Ashley EA, Bers DM, Robbins RC, Longaker MT, Wu JC. Abnormal calcium handling properties underlie familial hypertrophic cardiomyopathy pathology in patient-specific induced pluripotent stem cells. *Cell Stem Cell* 2013;**12**(1):101-13.
4. Lian X, Hsiao C, Wilson G, Zhu K, Hazeltine LB, Azarin SM, Raval KK, Zhang J, Kamp TJ, Palecek SP. Robust cardiomyocyte differentiation from human pluripotent stem cells via temporal modulation of canonical Wnt signaling. *Proc Natl Acad Sci U S A* 2012;**109**(27):E1848-57.
5. Wu H, Lee J, Vincent Ludovic G, Wang Q, Gu M, Lan F, Churko Jared M, Sallam Karim I, Matsa E, Sharma A, Gold Joseph D, Engler Adam J, Xiang Yang K, Bers Donald M, Wu Joseph C. Epigenetic regulation of phosphodiesterases 2A and 3A underlies compromised β -adrenergic signaling in an iPSC model of dilated cardiomyopathy. *Cell Stem Cell* 2015;**17**(1):89-100.
6. del Alamo JC, Meili R, Alvarez-Gonzalez B, Alonso-Latorre B, Bastounis E, Firtel R, Lasheras JC. Three-dimensional quantification of cellular traction forces and mechanosensing of thin substrata by fourier traction force microscopy. *PLoS One* 2013;**8**(9):e69850.

SUPPLEMENTAL TABLES

Table S1. Summary of iPSC lines and patient information in the current study

Group	Age	Gender	Pathogenic variants	Disease	LV EF	WT (sept/post)	DD grade	LAI ^b (ml/m ²)	E' (med/lat)	E/e'	E/A	TR vel	Comments
Ctrl	43	female	N/A	N/A	>50	N/A	N/A	N/A	N/A	N/A	N/A	N/A	healthy
	45	female	N/A	N/A	>50	N/A	N/A	N/A	N/A	N/A	N/A	N/A	healthy
HCM mutation carriers	57	female	MYH7 P.Arg663His (c.1988G>A)	HCM ^a	73	14/8	I	23	4.7/6	14.4	0.86	2.5	Exertional chest pain, Occasional PVCs
	25	male	MYH7 P.Arg663His (c.1988G>A)	none	61	11-Nov	none	30	10.8/12.9	5.3	1.4	2.2	
	62	female	MYBPC3 p.Val219Leu (c.655 G>C)	HCM ^a	70	17/13	II	64	3.2/4.2	22.6	0.66	n/a	
	42	female	MYBPC3 p.Val321Met (c.961G>A)	HCM ^a	49	18/13	I	41	6.1/8	8.5	1.4	2.1	
	46	female	MYBPC3 IVS27+1G>A (c.2905+1G>A)	HCM ^a	68	8-Dec	none	24	13/16.5	7.4	1.6	2.5	Exertional chest pain
	67	female	TNNT2 p.Arg92Trp (c.274 C>T)	HCM ^c	55	12/11	III	156	5.7/8.2	13.5	3.6	3.4	Restrictive physiology
	54	male	TNNT2 p.Arg92Trp (c.274 C>T)	HCM ^b /RCM	52	13/13	III	59	6.7/7.3	14.1	3.1	3	Restrictive physiology

Abbreviation: HCM, hypertrophic cardiomyopathy; LAI, left atrial volume index (ml/m²); LVEF, left ventricular ejection fraction; RCM, restrictive cardiomyopathy.

a: Reverse Curvature HCM;

b: Neutral HCM;

c: Apical HCM.

Table S2. Taqman® assay primers used in the current study

No.	Gene name	Assay ID	No.	Gene name	Assay ID
1	18S rRNA	Hs99999901_s1	12	PLN	Hs01848144_s1
2	GAPDH	Hs02786624_g1	13	CASQ2	Hs00154286_m1
3	SCN5A	Hs00165693_m1	14	RYR2	Hs00892883_m1
4	SCN7A	Hs00161546_m1	15	ATP2A2	Hs00544877_m1
5	CACNA1C	Hs00167681_m1	16	JPH2	Hs00375310_m1
6	CACNA1G	Hs00367969_m1	17	CAMK2A	Hs00947041_m1
7	SLC8A1	Hs01062258_m1	18	CAMK2D	Hs00943550_m1
8	MYH7	Hs01110632_m1	19	ITPR1	Hs00181881_m1
9	MYH6	Hs01101425_m1	20	NPPA	Hs00383230_g1
10	CAV3	Hs00154292_m1	21	NPPB	Hs00173590_m1
11	TNNT2	Hs00943911_m1			

Table S3. DNA oligos designed for CRISPR/Cas9 genome editing

Genome editing		TNNT2 R92W introduction	TNNT2 R92W correction
gRNAs	Forward	5' <u>CACC</u> Ggtccttccatgcgcttc 3'	5' <u>CACC</u> Gtccacccacaggacatccac 3'
	Reverse	5' <u>AAAC</u> gaagcgcacggagaaggacC 3'	5' <u>AAAC</u> gtggatgtcctgtgggtggaC 3'
ssODNs		5' ggggggtgtctagcccacccatctctctctgga ctctttggagtggcagcctctgagccgacgcggt ccaccacaggacatccacTggaagcgcacg agaaggacctgaatgagttgcaggcgt 3'	5' ggggggtgtctagcccacccatctctctctgga ctctttggagtggcagcctctgagccgacgcggt ccaccacaggaCatAcaTCggaagcgcacg gagaaggacctgaatgagttgcaggcgt 3'
Sequencing primers	Forward	5' cccaagcaaagccagcctgact 3'	5' cccaagcaaagccagcctgact 3'
	Reverse	5' tgcccgaccttctcacttctcca 3'	5' tgcccgaccttctcacttctcca 3'

Underlined: Restriction site for the cloning

Red: Nucleotide to be replaces

Blue: Same-sense mutations in ssODN template to avoid repeated cutting of gRNAs

Table S4. Summary of N number, control group, and statistical methods in the figures

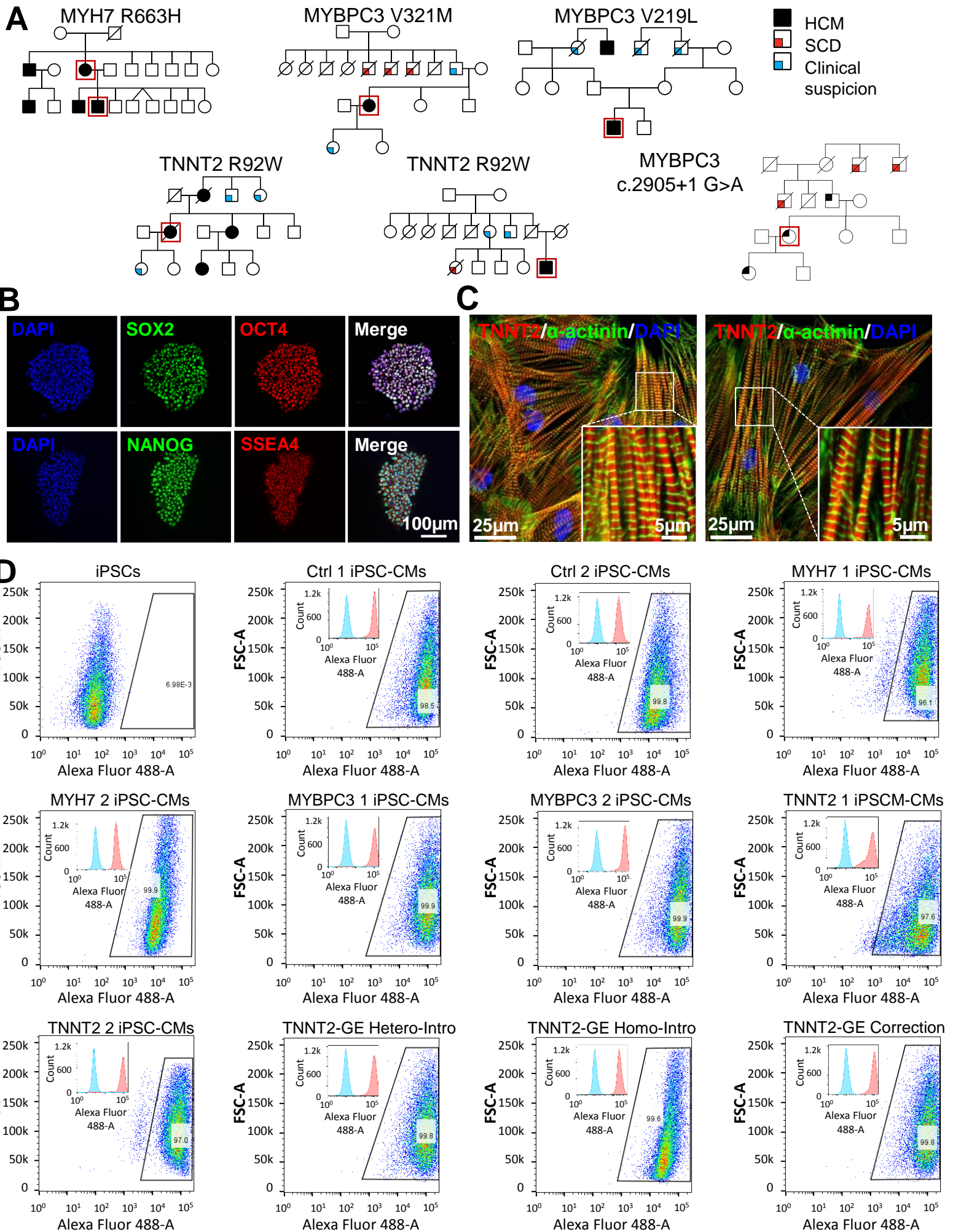
Data set		Control group	N number of experiments (per group)					Method of statistics	
			Cell experiments			Other experiments		Test	After test
Figure	Panel		N of Cells	¹ N of Lines	² N of batches	Bio Repeats	Tech Repeats		
Figure 1	D - G	Ctrl	42, 36, 40, 44 ³	2	3			1-way ANOVA	Tukey
Figure 2	B - C	Ctrl	51, 42, 43, 72	2	3			1-way ANOVA	Tukey
Figure 2	E - F	Ctrl	22, 28, 25, 26	2	2			1-way ANOVA	Tukey
Figure 3	E - H	Ctrl	77, 190, 192, 64	2	3			1-way ANOVA	Tukey
Figure 4	B - C	Base	51, 47, 42, 41, 43, 33, 72, 41	2	3			2-way ANOVA	Sidak
Figure 4	D	Base	48, 41, 33, 28, 36, 42, 30, 32	2	3			Z test	
Figure 4	F - I	Base	42, 33, 36, 30, 40, 28, 44, 29	2	3			2-way ANOVA	Sidak
Figure 5	B - C	Baseline	51, 42, 35, 62, 43, 51, 28, 72, 30, 33, 29, 32, 60	2	3			2-way ANOVA	Tukey
Figure 5	D - F	Baseline	42, 35, 30, 27, 29, 40, 21, 30, 29, 44, 40, 34, 35	2	3			2-way ANOVA	Tukey
Figure 6	A	Ctrl		2	2	3	3	1-way ANOVA	Tukey
Figure 6	B	Ctrl, HCM		2	2	3	2	1-way ANOVA	Tukey
Figure 6	C - D	ISO Ctrl	50, 81, 105, 101, 108, 93, 105	2	2			1-way ANOVA	Tukey
Figure 6	E - F	Baseline		2	2	3	2	Student's t-test	
Fig. S2	A - D	Ctrl	42, 36, 40, 44	2	3			1-way ANOVA	Tukey
Fig. S3	B - D	0.5 HZ	12, 16, 18, 10, 11	1	2			1-way ANOVA	Tukey
Fig. S4	B - E	Ctrl	163, 152	2, 1	2, 3			Student's t-test	
Fig. S4	F - I	Ctrl	46, 51	2, 1	2, 2			Student's t-test	
Fig. S5	G - I	Ctrl, HCM	163, 127, 139, 129, 123	1	3			1-way ANOVA or Student's t-test	Tukey
Fig. S5	J - L	Ctrl, HCM	42, 62, 68, 44, 78	1	3				
Fig. S6	B - F	Ctrl	74, 72, 59	2, 2, 1	2			1-way ANOVA	Tukey
Fig. S7	A - B	Base	51, 47, 42, 41, 43, 33, 72, 41	2	3			2-way ANOVA	Sidak
Fig. S7	C - D	Base	42, 33, 36, 30, 40, 28, 44, 29	2	3			2-way ANOVA	Sidak
Fig. S8	B - D	HCM base	51, 72, 114, 94, 100	2	2			1-way ANOVA	Tukey
Fig. S8	E - G	HCM base	42, 44, 36, 28, 32	2	2			1-way ANOVA	Tukey
Fig. S9	A	Ctrl		2	2	3	3	1-way ANOVA	Tukey
Fig. S9	B	None		2	2	3	2	None	
Fig. S9	F - H	Ctrl treated	50, 52, 52, 31, 54, 41, 106, 34	2	2			2-way ANOVA	Tukey
Fig. S10	A	Ctrl NC, HCM SINC		2	2	3	3	Student's t-test	
Fig. S10	B	Ctrl		2	2	3	2	Student's t-test	
Fig. S10	C	HCM		2	2	3	2	Student's t-test	
Fig. S10	E - G	Ctrl WT, HCM NC	52, 89, 73, 64	2	2			Student's t-test	
Fig. S10	H - J	Ctrl WT, HCM NC	46, 45, 48, 52	2	2			Student's t-test	
Fig. S10	K	Base		2	2	3	2	2-way ANOVA	Tukey

1: the number of patient specific iPSC-CM lines used for each experiments;

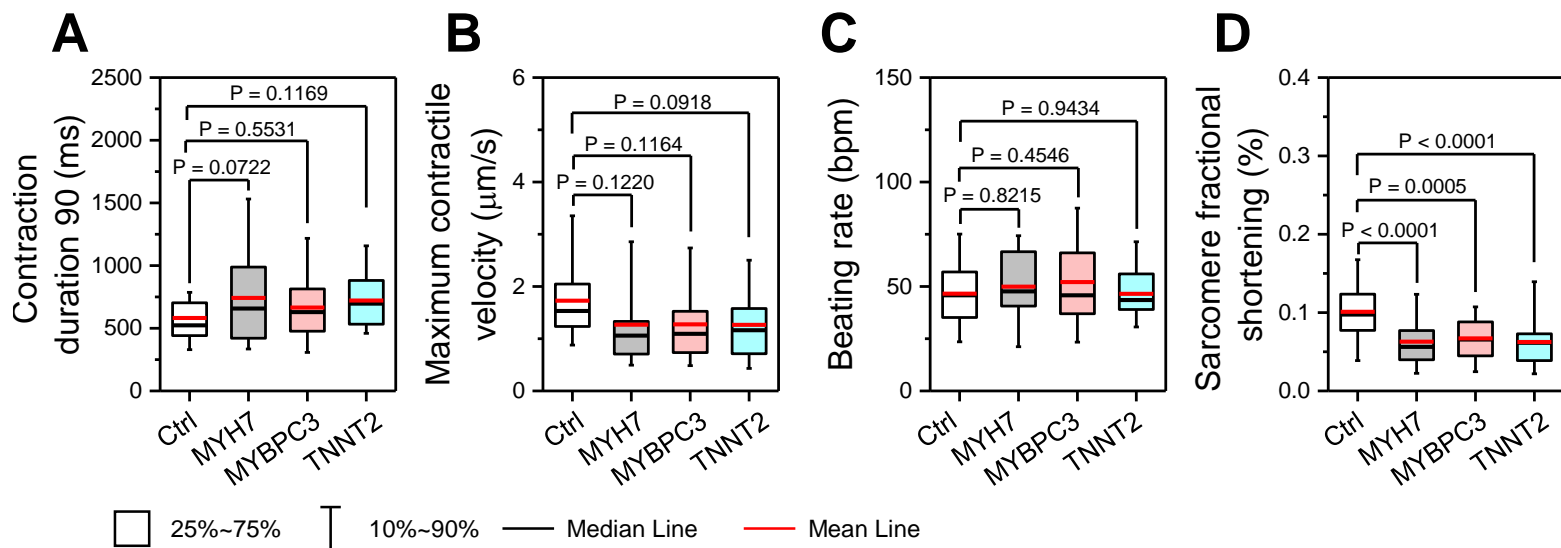
2: the number of batches of iPSC-CM differentiation that were performed for each line;

3: the number of each groups follows the order of group appearance. In the indicated cell, 42, 36, 40, 44 represented n = 42, 36, 40, 44 cells in Ctrl, MYH7, MYBPC3, and TNNT2 groups, respectively.

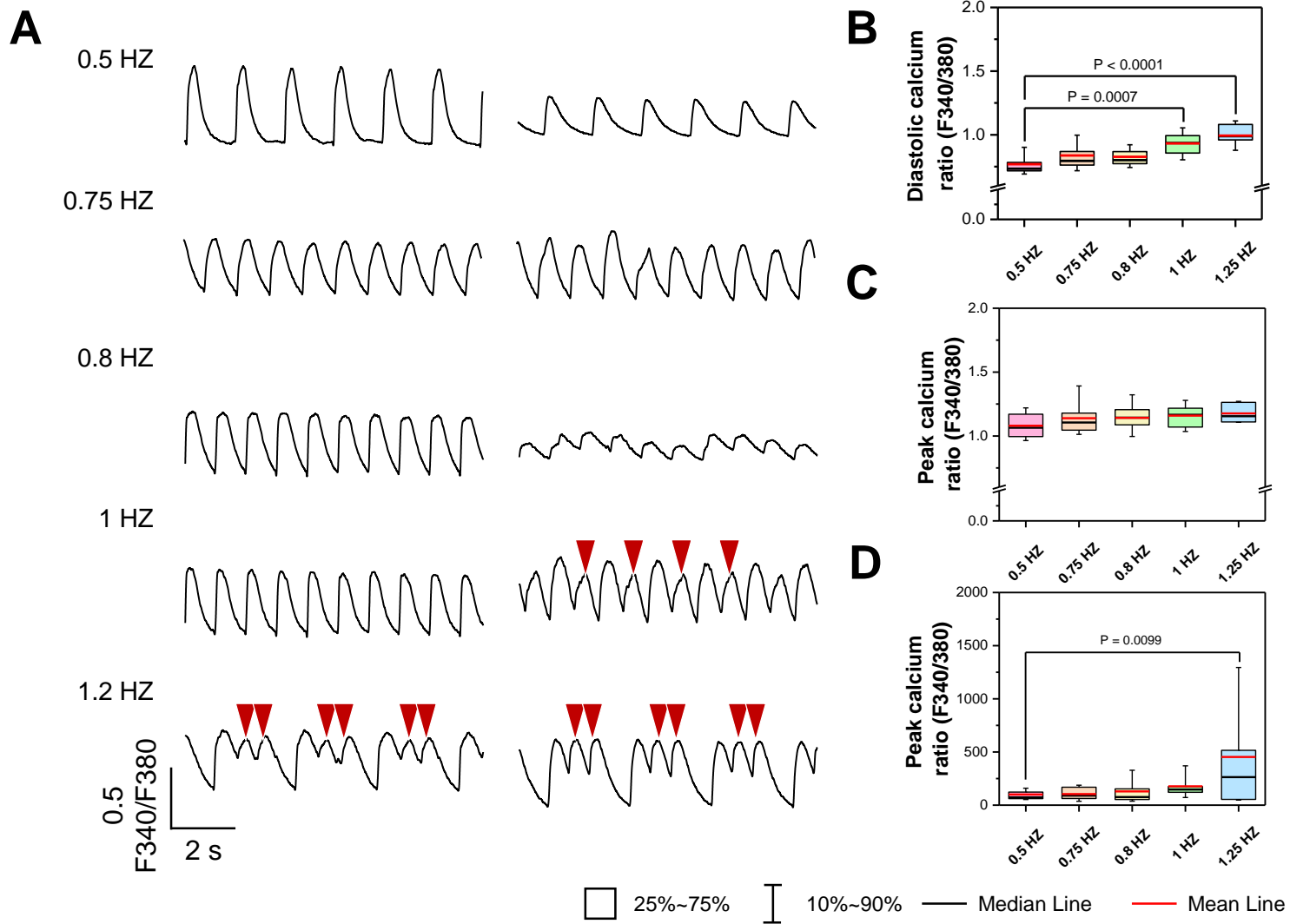
Supplemental Figure 1. Differentiation of patient specific HCM iPSC-CMs.



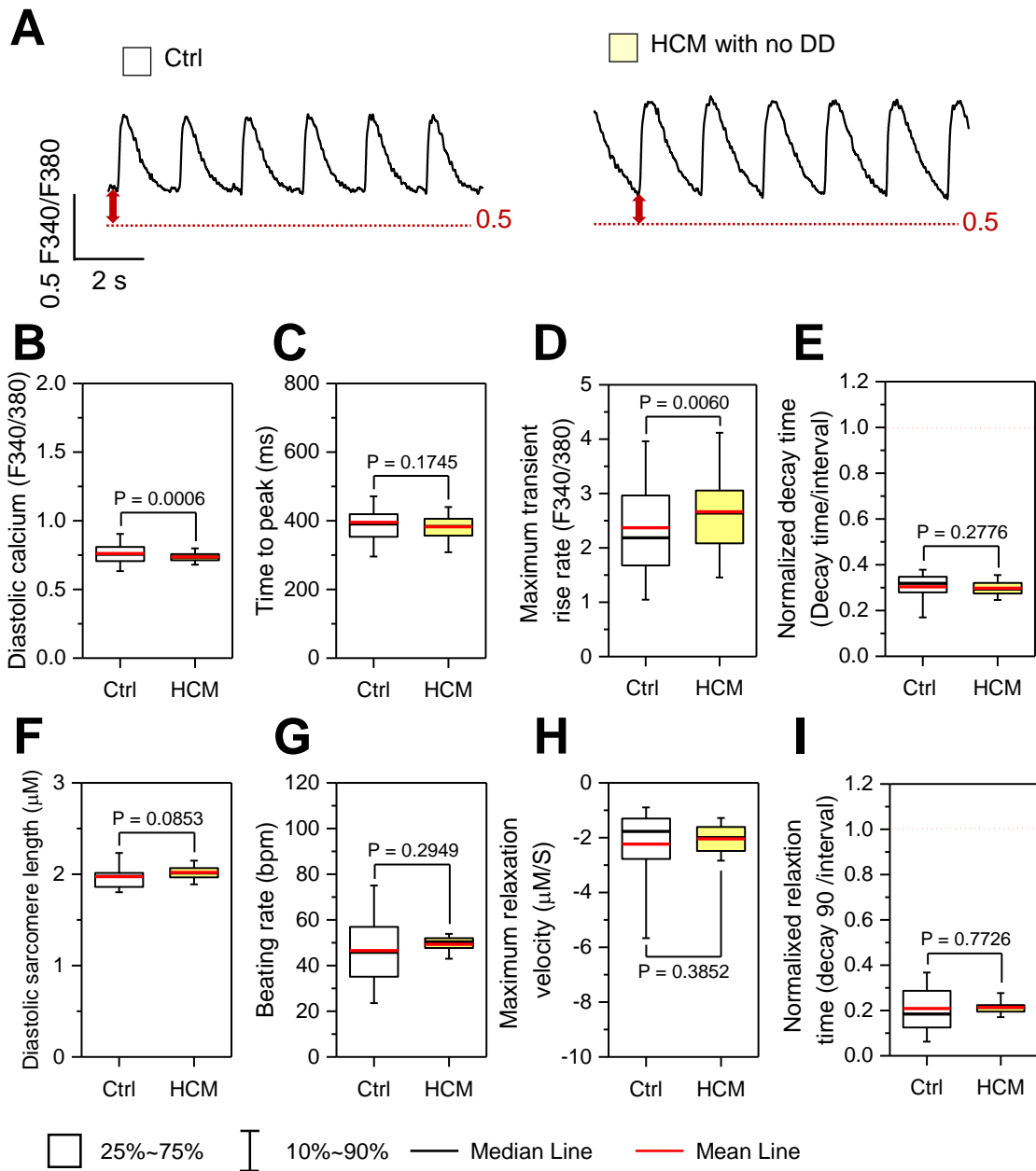
Supplemental Figure 2. Recapitulation of diastolic dysfunction in patient-specific HCM iPSC-CMs.



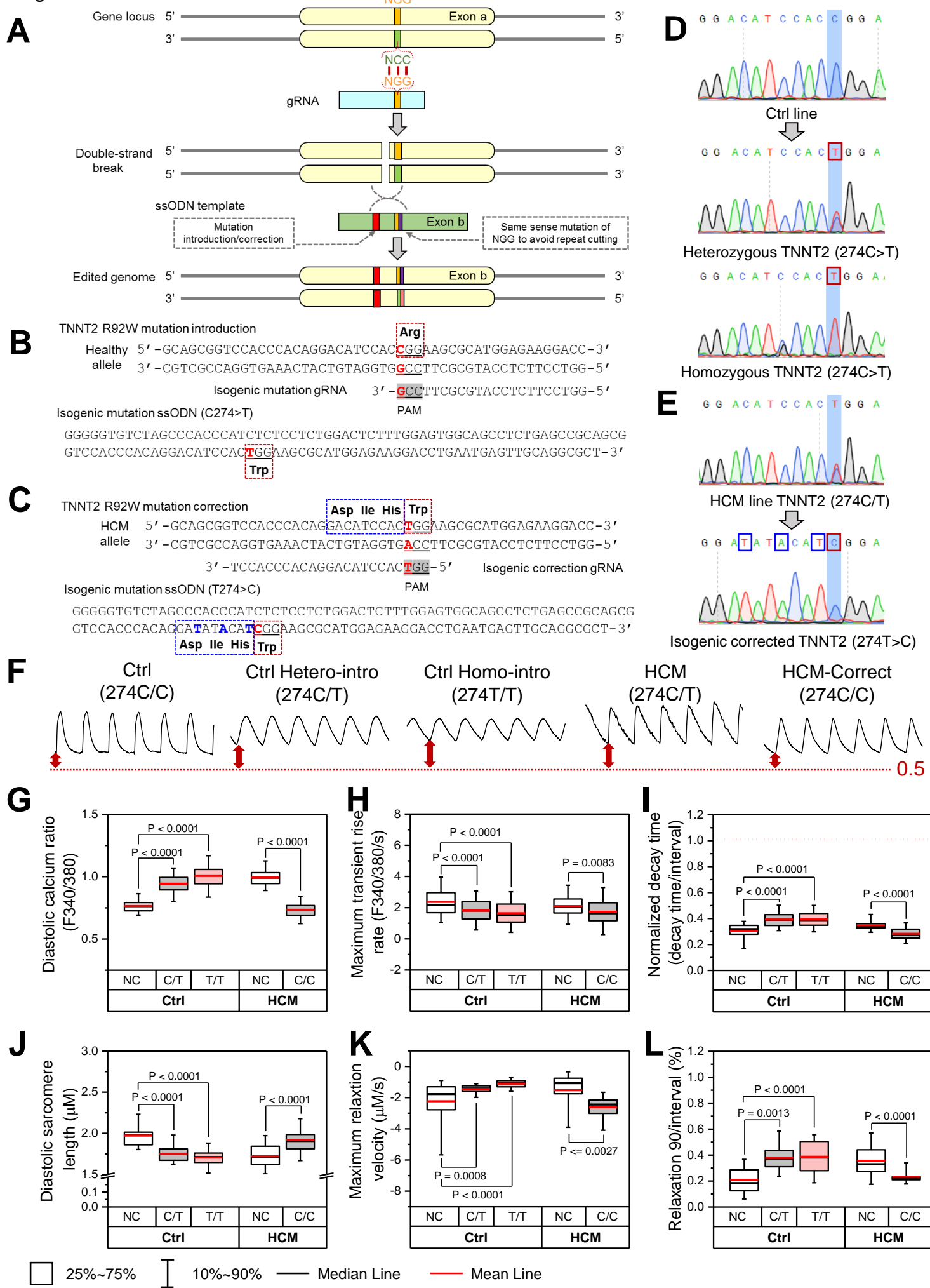
Supplemental Figure 3. Optimization of Fura-2 AM ratiometric Ca²⁺ imaging.



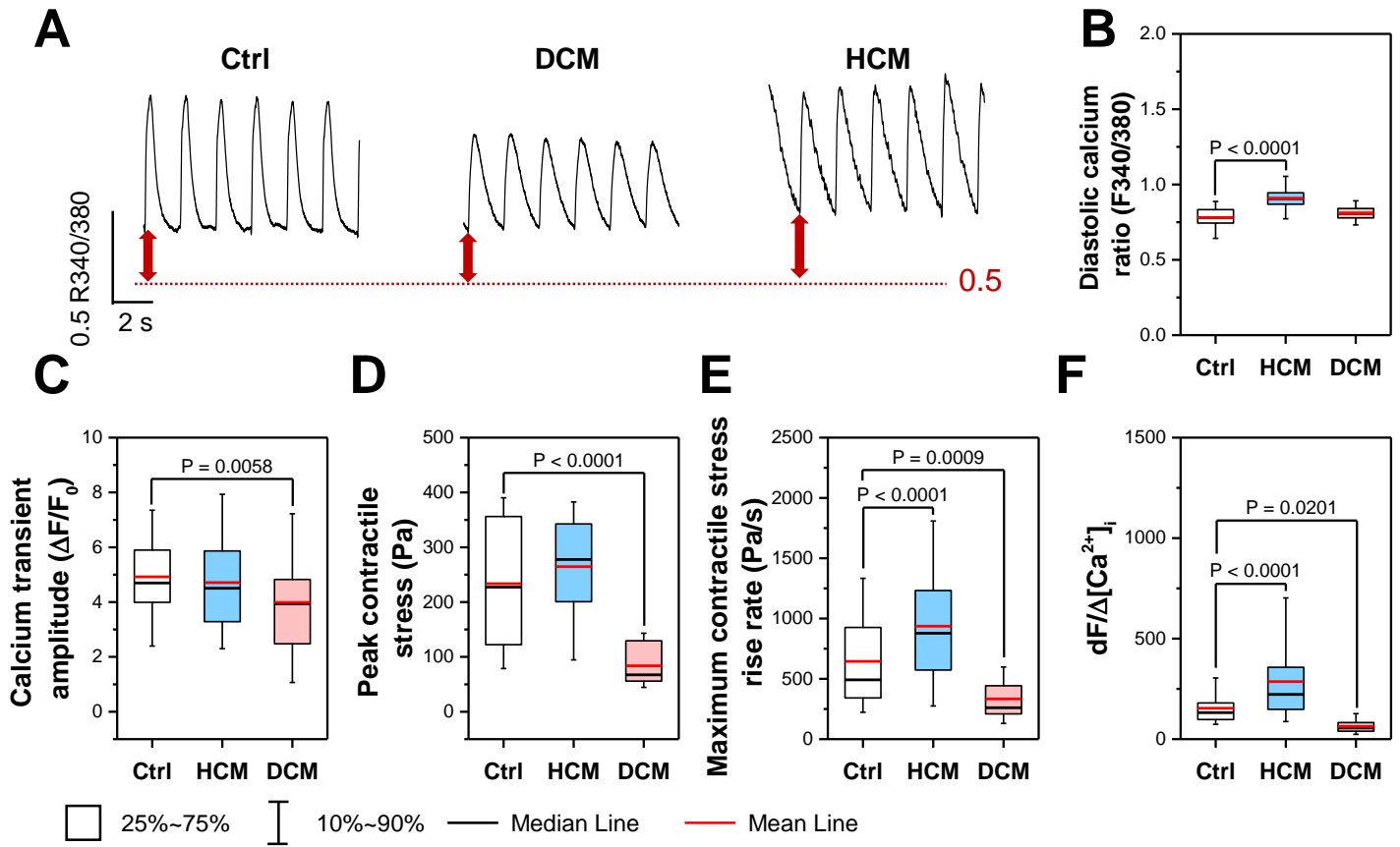
Supplemental Figure 4. iPSC-CMs from HCM patient without DD showed normal diastolic function.



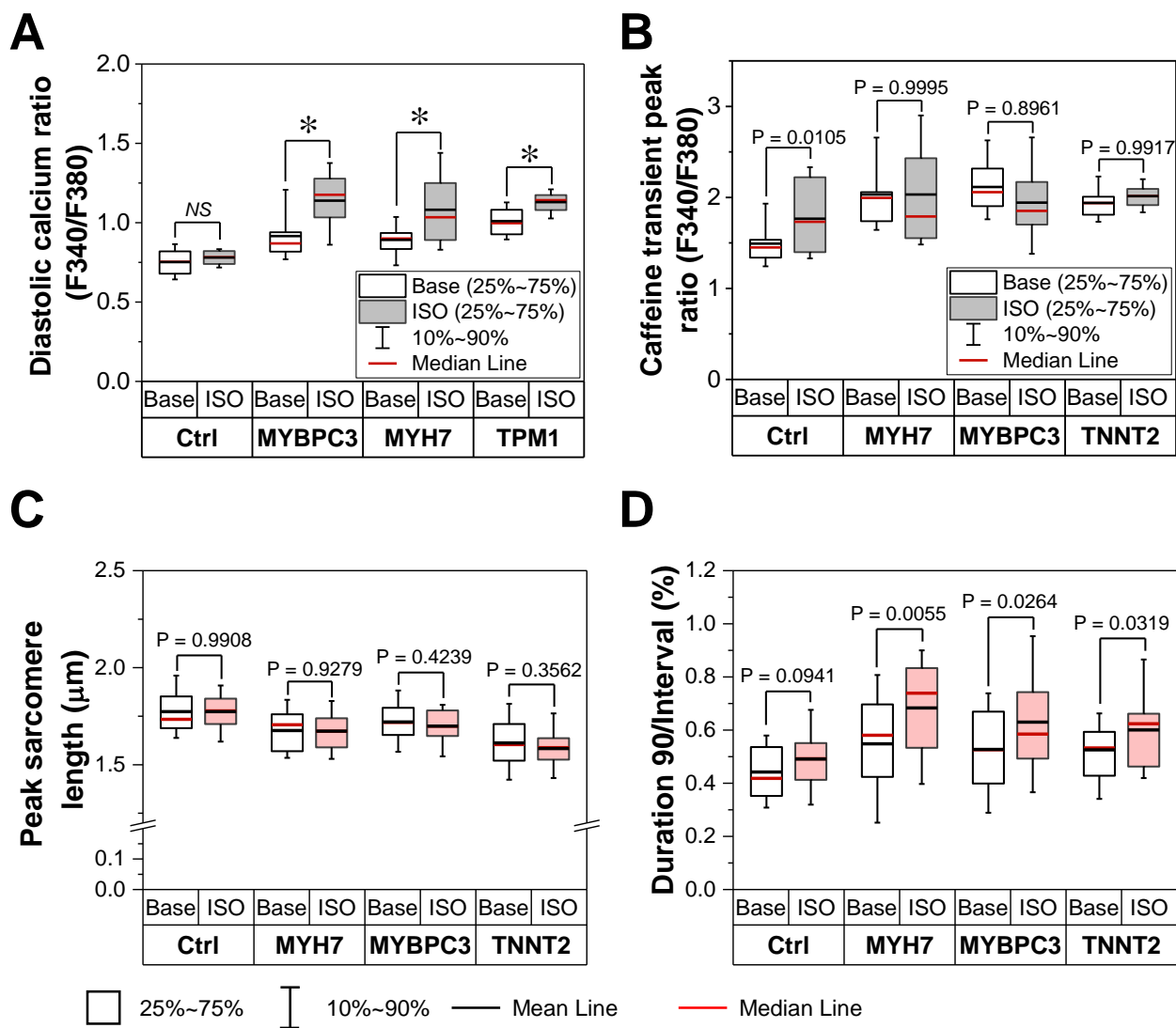
Supplemental Figure 5. Confirm the pathogenicity of HCM mutation using CRISPR/Cas9-edited isogenic Ctrl and HCM iPSC line.



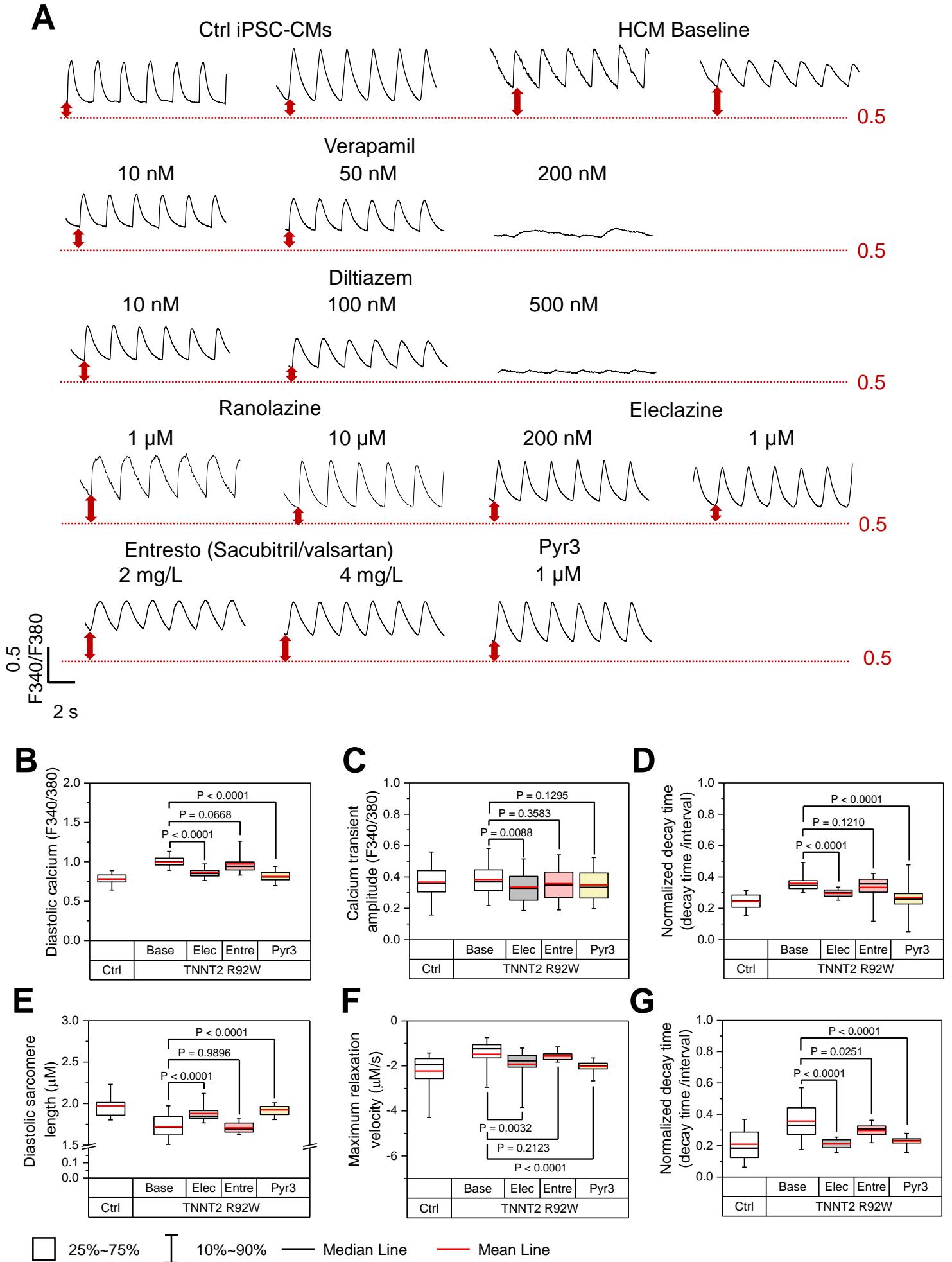
Supplemental Figure 6. DCM and HCM iPSC-CMs showed opposite changes in Ca^{2+} sensitivity.



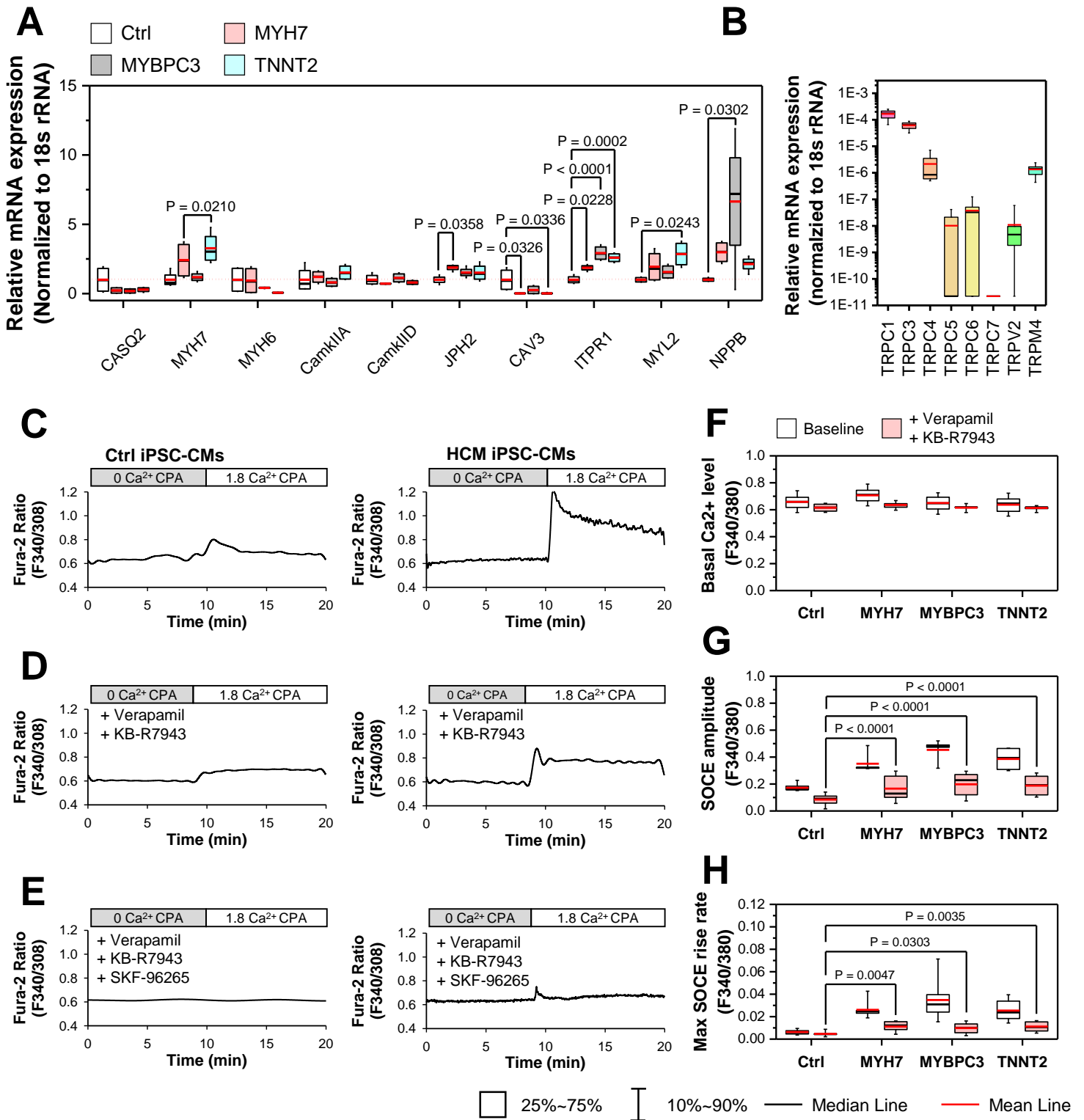
Supplemental Figure 7. Short-term β -adrenergic stimulation exaggerated Ca^{2+} overload and slow relaxation in HCM iPSC-CMs.



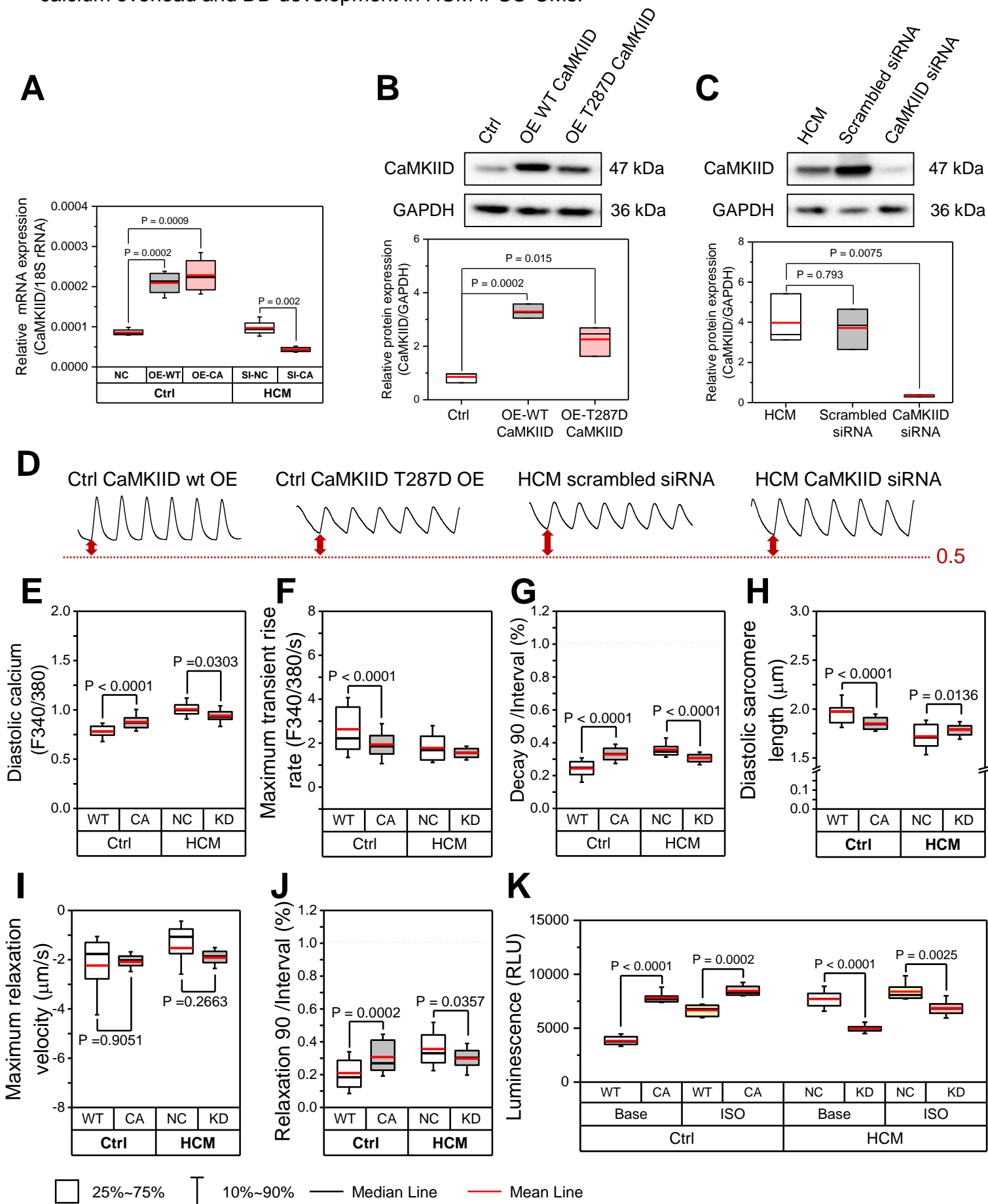
Supplemental Figure 8. Treatment of HCM iPSC-CMs with Ca²⁺ and late Na⁺ channel blockers.



Supplemental Figure 9. Up-regulation of TRPCs contribute to the increase of SOCE in HCM iPSC-CMs.

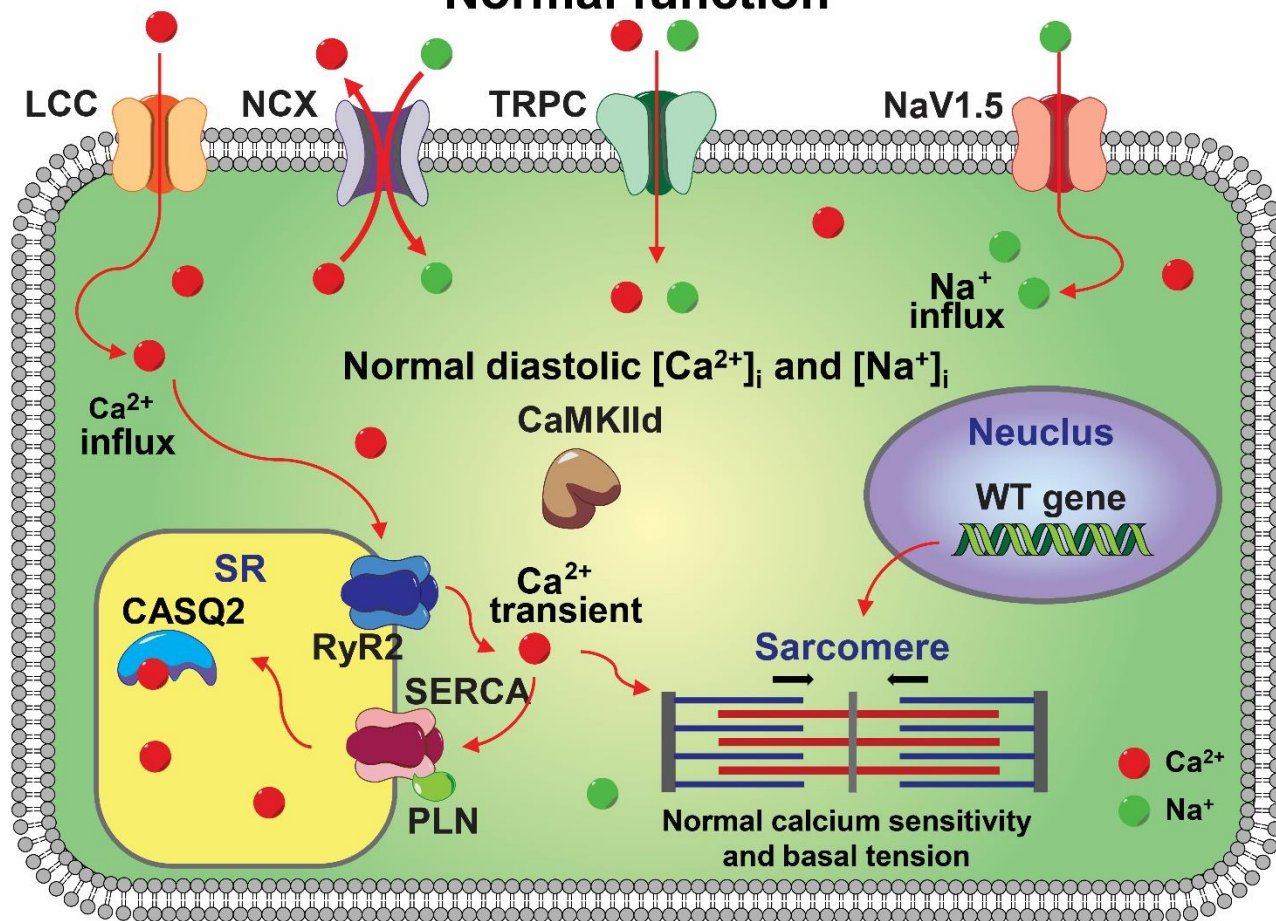


Supplemental Figure 10. Gain and loss-of-function study confirmed the key role of CaMKII δ activation in calcium overload and DD development in HCM iPSC-CMs.



Supplemental Figure 11. Schematic diagram of the cellular mechanisms of diastolic dysfunction in HCM iPSC-CMs.

Normal function



Diastolic dysfunction

